Impact of the Mission Profile Length on Lifetime Prediction of PV Inverters

A. F. Cupertino, J. M .Lenz, H. A. Pereira, S. I. Seleme Jr E.M . S. Brito and J.R. Pinheiro

Impact of the Mission Profile Length on Lifetime Prediction of PV Inverters

Allan F. Cupertino*[a,b], João M. Lenz[c], Erick M. S. Brito[b], Heverton A. Pereira[d], José R. Pinheiro[c], Seleme I. Seleme Jr.[b]

[a]Department of Materials Engineering, Federal Center for Technological Education of Minas Gerais, Belo Horizonte - MG, Brazil
[b]Graduate Program in Electrical Engineering - Federal University of Minas Gerais, Belo Horizonte, MG, Brazil
[c]Power Electronics and Control Research Group (GEPOC), Federal University of Santa Maria – UFSM, Santa Maria, RS, Brazil
[d]Department of Electrical Engineering, Federal University of Viçosa, Viçosa, MG, Brazil

Abstract

The first step of the design for reliability (DFR) approach in PV inverters is the translation of the mission profile into thermal loading. Most works employ only a one-year mission profile even though it is known that it changes year to year due to climatic reasons and randomness of cloud behavior. This work evaluates how mission profile length affects the system-level reliability of a 5.5 kW PV inverter. Different mission profile lengths (1-5 years) are compared to the typical average year (TAY) mission profile. The results indicate that the use of 1 year mission profile affects by 7 % the estimated inverter B_{10} lifetime.

Keywords: Photovoltaic Systems, Mission profile, Lifetime Estimation, System-level Reliability.

1. Introduction

The installed power of grid-connected photovoltaic (PV) systems has increased considerably in the recent years. In order to inject the generated power into the grid, PV inverters are usually employed. The PV inverter must have a high conversion efficiency and fulfill the requirements of the modern grid codes. Fig. 1 shows the structure of a single-phase grid connected PV inverter. This topology is widely employed in residential PV systems.
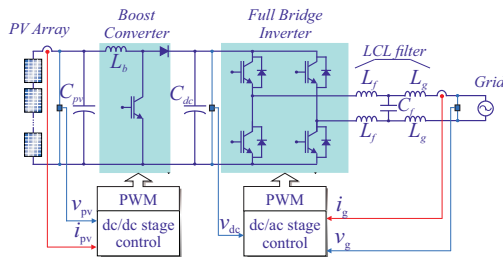
Figure 1: Schematic of a single-phase PV inverter with LCL filter.

Real field experience based surveys indicate that the PV inverter causes many of the failures in photovoltaic systems [1]. Industrial surveys show that semiconductor devices and electrolytic capacitors are the weakest components in electronic systems [2, 3]. Unexpected and frequent failures in PV systems increase the cost of energy due to unscheduled maintenance and/or replacement. In order to improve the competitiveness of the PV systems in the energy market and reduce the cost of generated energy, more reliable PV inverters must be designed. Therefore, reliability evaluation methodologies have been widely employed in photovoltaic systems in recent years [4].

The mission profile based lifetime estimation is an important tool for the reliability evaluation of electronic systems [5]. Thermal stresses are among the main causes of failures in semiconductor devices and capacitors [3]. Therefore, this methodology translates the mission profile into thermal stresses in the components. The damage in the components can be evaluated based on lifetime models obtained from accelerated life tests [6].

Reference [7] presented a methodology to predict the bond wire fatigue of the IGBTs in a 10 kW 3-phase inverter. A mission profile based lifetime estimation is implemented using one-year temperature and irradiance mission profiles. The analysis is followed by a Monte Carlo simulation. The system-level reliability theory is used to combine the effect of individual components. Based on this methodology, other papers discussed

---

Email address: `Corresponding Author:`
`afcupertino@ieee.org` (Allan F. Cupertino*)

the important factors which affect PV inverter lifetime [8, 9, 10, 11].

Reference [8] evaluates how the PV panel degradation rate and installation site affect the PV inverter lifetime. In [9], the oversize of the PV array with respect to the inverter rated power is investigated and the effect on lifetime is evaluated. In these references, only the dc/ac stage is taken into account. The effect of the photovoltaic module characteristics on PV micro-inverters lifetime is discussed in [10]. Only the dc/dc stage power semiconductors are considered. Reference [11] proposed the mission profile-oriented control in order to increase the reliability of PV inverters. Recently, reference [12] evaluated the lifetime of a PV micro-inverter, taking into account both dc/dc and dc/ac stages.

Regarding the role of the mission profile data, reference [13] proposes a methodology to characterize the mission profile of photovoltaic systems, considering different panel orientations and different types of mechanical tracker. The effect of the mission profile resolution on lifetime estimation is discussed in [4]. Furthermore, the effect of the mission profile perceptual variations and the thermal dynamics of the PV panels are analyzed in [14].

All the references aforementioned consider an one-year mission profile. The analysis assumes that the mission profile would be identical in all years of operation. Nevertheless, it can change from year to year due to climatic reasons and randomness of cloud behavior. The effect of the mission profile length (number of distinct years) on the estimated lifetime of PV inverters has not been discussed in the literature yet. Therefore, this work aims to fill this void and provide the following contributions:

- Analysis of the PV inverter lifetime for different mission profile lengths;

- Benchmarking of the lifetime estimation for different mission profile lengths and typical average year mission profile;

- Lifetime evaluation of a PV inverter, considering semiconductors and capacitors of both dc/dc and dc/ac stages.

The typical average year (TAY) is a one-year mission profile obtained by averaging the variables (solar irradiance and ambient temperature) according to the time in which these data were measured, i.e. 5 years. Thus, TAY values are the representative average condition of each variable throughout the year [13].

This paper is outlined as follows. Section 2 presents the reliability evaluation procedure of the PV inverter. Section 3 describes the mission profiles employed in the study. The obtained results are presented in Section 4 and the conclusions are stated in section 5.

2. Mission profile based lifetime evaluation

The lifetime estimation approach adopted in this paper considers the power devices and the electrolytic capacitors. The methodology is summarized in Fig. 2 and can be divided into three steps: Thermal loading evaluation, static damage computation and Monte Carlo simulation.

2.1. Power Semiconductors

The flowchart for power semiconductor lifetime estimation is presented in Fig. 2 (a). The junction temperatures of the semiconductor devices are estimated based on the methodology presented in [9]. Look-up tables of the conduction and switching losses provided by the manufactures are employed [15]. The calculated power losses are applied to the thermal model of each device. The thermal dynamics of each device is expressed by the Foster model of the junction-to-case (Z_{j-c}), case-to-heatsink (Z_{c-h}) and heatsink-to-ambient (Z_{c-h}) thermal impedances. All the IGBTs and diodes are considered to be in the same heatsink.

The thermal loading can be classified as long-cycle periods (related to the mission profile variations) and short-cycle periods (related to the grid frequency) [16]. All the PV inverter power devices are subjected to long thermal cycles, due to variations in the PV array generated power. However, the elements of the full-bridge inverter perform the dc/ac conversion, which results in additional short thermal cycling. This fact is not experienced by the boost converter elements, since at this stage only the dc/dc conversion is performed.

For the long-cycling analysis, the rainflow algorithm is used to convert the irregular thermal cycles into a set of cycles with defined average temperature $T_{j,m}$, cycle amplitude ΔT_j and heating time t_{on}. This procedure is necessary, since most of the lifetime models consider well defined cycles. For the short-cycling analysis, the average temperature is the same as that of the rainflow algorithm. The heating time is assumed to be equal to half of the grid period. Finally, the cycle amplitude is computed through the analytical model proposed by [16].

Based on the thermal loading information, the number of cycles to failure can be computed as follows [17]:
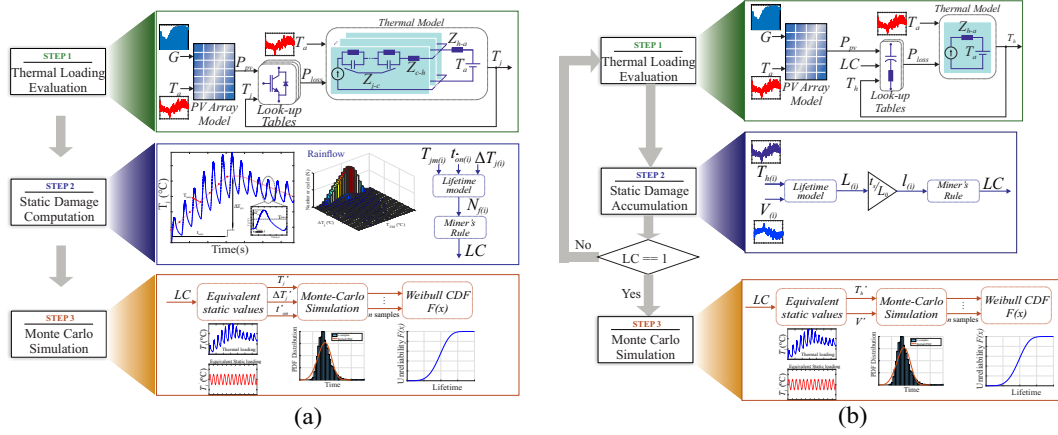
Figure 2: Mission profile based lifetime evaluation: (a) Approach for the power semiconductor devices; (b) Approach for the dc-link and input capacitors.

$$N_f = A(\Delta T_j)^\alpha (ar)^{\beta_1 \Delta T_j + \beta_0} \left[\frac{C + (t_{on})^\gamma}{C + 1} \right] \exp\left(\frac{E_a}{k_b T_{jm}} \right) f_d. \tag{1}$$

where the parameters A, α, β_0, β_1, C, γ and f_d are obtained from the curve fitting of power cycle tests and can be found in [17]. $ar = 0.31$ is considered in the present work. The accumulated damage due to the mission profile can be computed by using the Miner's rule, as follows:

$$LC = \sum_i^n \frac{1}{N_{f,i}}, \tag{2}$$

where n is the total number of thermal cycles.

The inverse value of the damage computed in (2), however, cannot be interpreted as the converter lifetime, since the power modules are not identical and the failures can happen at different times. Therefore, a statistical analysis is usually necessary. Initially, the stochastic parameters ΔT_j, t_{on} and T_{jm} are converted into equivalent deterministic static values, denoted by $\Delta T'_j$, t'_{on} and T'_{jm} using the methodology proposed by [7]. The thermal loading on the power devices are dependent on the collector-emitter voltage (V_{CE}), provided by manufacturers. In addition, the maximum variation of V_{CE} can also be found in the datasheet, given an estimation of how the thermal loading parameters, ΔT_j and T_{jm} vary as a response of V_{CE}. Finally, the technology factor A is also varied up to ±20%, representing manufacturing process uncertainties.

Then, a Monte Carlo simulation with 10000 samples is performed and its output is the distribution of the power device lifetime, which usually follows a Weibull distribution:

$$f(x) = \frac{\beta}{\eta^\beta} x^{\beta-1} exp\left[-\left(\frac{x}{\eta} \right)^\beta \right], \tag{3}$$

where β is the shape parameter, η is the scale parameter and x is the operation time.

Finally, the reliability of one power device can be evaluated by considering the Cumulative Density Function (CDF) $F(x)$ of the Weibull distribution, given by:

$$F(x) = \int_0^x f(x)dx. \tag{4}$$

$F(x)$ is usually referred as unreliability function.

2.2. Capacitors

The flowchart for the capacitor lifetime estimation is presented in Fig. 2 (b). According to [18], a common used lifetime model of aluminium electrolyte capacitors is given by:

$$L_f = L_0 \left(\frac{V_c}{V_n} \right)^n 2^{\frac{T_h - T_n}{10}}. \tag{5}$$

where n is usually in the range of $1 \leq n \leq 5$ [18]. In the present paper, $n = 1$ is used. L_0 is the capacitor nominal lifetime (usually in hours) under the voltage V_n and temperature T_n. Voltage and temperature are important stress factors. Voltage stress in the dc-link capacitor (C_{dc}) is assumed constant in reason of the voltage controller employed; while the voltage in the inverter input capacitor (C_{pv}) is the PV array's calculated maximum power point.

3

The hot-spot temperature of the capacitors is computed considering the frequency and the temperature dependence of its equivalent series resistance (ESR), as discussed in [19]. Look-up tables are employed to increase the speed of this process. Additionally, the dependence on ESR and damage are also analyzed. Then, the total damage in the capacitors is computed through the Miner's rule, as follows:

$$LC = \sum_{i}^{m} l_i = \sum_{i}^{m} \frac{t_{mp}}{L_i}, \qquad (6)$$

where t_{mp} is the mission profile sample time and m is the number of samples of the mission profile. L_i is the lifetime computed by eq. (5) during each mission profile sample.

The estimated static damage given by (6) underestimates the capacitor damage, since ESR is expected to increase over time (due to degradation). This degradation process in ESR increases the thermal stress and consequently reduces lifetime. In order to make a more conservative lifetime estimation, a simplified degradation approach is used. A common failure criterion for capacitors provided by manufacturers is to assume that the ESR reaches the double of its initial value. This reasoning suggests the following degradation formula:

$$ESR_i = (1 + LC) ESR_{i-1}, \qquad (7)$$

which guarantees that the ESR reaches the double of its initial value at the end of life. It is important to note that eq. (7) is a rough estimate of the degradation process. Nevertheless, the approach is conservative since experimental results presented in [20] suggests a slow degradation rate. A more precise degradation model estimation can be reached through the experimental characterization of a given part number. However, this is beyond the scope of this paper.

In electrolytic capacitors, the thermal stress is caused by the power dissipation on the ESR. Thus, a variation of ±20% in the ESR value is performed to obtain the maximum variation of the static hot-spot temperature T_h. Finally, a variation of ±15% in the rated useful life L_0 is considered, representing the manufacturing process uncertainties. Once the static damage is computed, Monte Carlo simulations with 10000 samples are used to compute the unreliability function of both C_{pv} and C_{dc}.

2.3. System Level Reliability

If a failure in any semiconductor device or capacitor occurs, the inverter performance and safe operation will be compromised. Therefore, these components are in series in the reliability block diagram. Accordingly, the system level reliability can be computed by:

$$F_{sys}(x) = 1 - \prod_{i=1}^{N_c} (1 - F_i(x)). \qquad (8)$$

where N_c is the number of components (power devices and capacitors) of the PV inverter. Then, it is possible to obtain the lifetime B_x, which refers to the time when $x\%$ of the samples have failed [7]. B_{10} is a common reliability metric used by manufacturers and design engineers.

3. Case Study

The lifetime evaluation methodology is exemplified considering a 5.5 kW single-phase inverter case study. The parameters of the inverter are presented in Table 1. The 4th generation IGBT part number IKW20N60T [15], rated at 25 A/600 V and manufactured by Infineon, is used in both inverter and boost converter. The aluminium electrolytic snap-in capacitors with part number B43522 and manufactured by TDK are employed in both inverter and boost converter capacitor banks. The dc-link capacitor bank C_{pv} consists in 3 capacitors of 1000 μF in parallel. The boost converter capacitor bank (C_{pv}) is based on 2 capacitors of 390 μF in parallel.

Table 1: Parameters of the PV inverter.

Parameter	Value
Grid voltage (line to line) V_g	220 V
Rated power S_n	5.5 kVA
Full bridge Switching frequency	12 kHz
LCL filter inductance ($L_f = L_g$)	0.5 mH
LCL filter capacitance (C_f)	6 μF
Dc-link Voltage v_{dc}	400 V
Dc-link capacitance C_{dc}	3000 μF
Boost converter inductance L_b	1.2 mH
Boost converter capacitance C_{pv}	780 μF
Boost converter switching frequency f_{sb}	12 kHz

The 5-year mission profiles adopted in this work are presented in Fig. 3 (a)-(b). These are composed of global solar irradiance and ambient temperature measurements from a weather station located in the Canary Islands. The sampling time is 1 minute. In

4

this work, a PV array of 2 parallel strings of 7 Kyocera KD250GX-LBF2 photovoltaic panels is connected to the PV inverter. The photovoltaic panel thermal dynamics is modeled by a first order system with time constant of 5 minutes [14]. The generated power mission profile under such conditions is presented in Fig. 3 (c). A profile of a typical operating day is also shown in the zoomed views of Fig. 3.
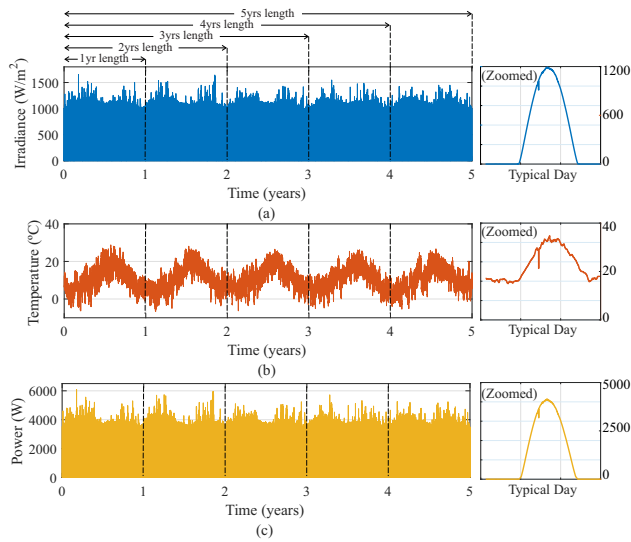
Figure 3: Mission profiles adopted for lifetime evaluation: (a) Solar irradiance; (b) Ambient temperature; (c) Power generated by the PV array.

The unreliability of each component is obtained by following the methodology previously described. The effect of the mission profile length on the system level B_{10} lifetime is evaluated. For the sake of comparison, the lifetime is initially evaluated considering only the first year of the real weather data mission profile and assuming this profile constant for the following operating years. The same approach is repeated, considering the first 2, 3, 4 and 5 years of the mission profile, as illustrated in Fig. 3, in order to show how the mission profile length affects B_{10} lifetime. Finally, the results are benchmarked with the TAY obtained according to [13].

4. Results

Figure 4 shows the thermal loading in all the PV inverter components for the 5-year mission profile, including a zoomed view of a typical operating day. As observed, the boost converter elements reach higher temperatures than those of the full bridge. Nevertheless, the full bridge components present both long and short-term thermal cycling, which contributes to accelerate the bondwire fatigue. Regarding the capacitor banks, the dc-link capacitors present higher temperatures than the input capacitors. This fact is related to the double line frequency harmonic ripple experienced by the dc-link capacitor, which considerably increases power losses.
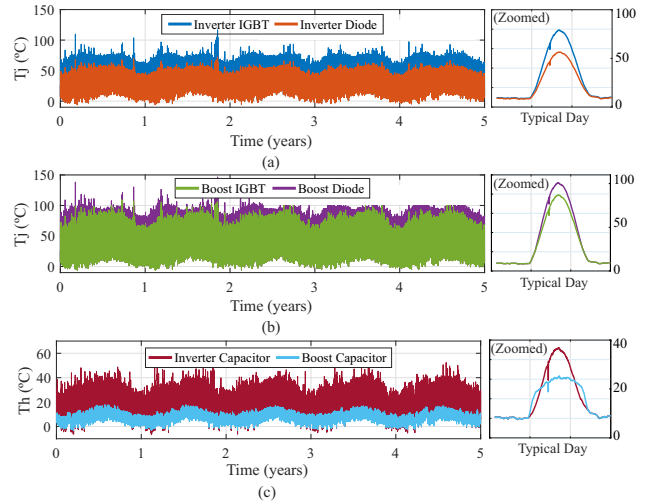
Figure 4: Thermal loading of the components of the PV inverter: (a) Full bridge IGBT and diode; (b) Boost converter IGBT and diode; (c) Dc-link and input capacitor.

The yearly static damage derived from the thermal loading for all the PV inverter components are presented in Table 2. As previously discussed, the boost semiconductors have lower static damage since they present only long-cycling stresses in comparison with the full bridge elements. In addition, the dc-link capacitor and the IGBT are notoriously the most stressed components, with higher static damage.

Table 2: Static damage computed for each dc/dc and dc/ac components (base of damage 10^{-3}).

MP length	dc/dc components			dc/ac components		
	IGBT	Diode	Cap	IGBT	Diode	Cap
1 year	0.035	0.059	6.35	15.8	0.131	19.1
2 years	0.028	0.058	6.23	16.4	0.028	18.8
3 years	0.027	0.053	6.24	16.9	0.027	19.0
4 years	0.025	0.052	6.24	16.7	0.138	19.1
5 years	0.027	0.055	6.22	16.9	0.139	19.0
TAY	0.013	0.024	6.31	11.2	0.096	17.9

The maximum deviations assumed in the Monte Carlo simulation are obtained based on a sensitivity analysis. The semiconductors collector-emitter voltage and the capacitors ESR are increased considering

the maximum margins provided by the manufacturer. Based on this, the perceptual variation in the static values in Table 2 is computed. The obtained increases in the static values are summarized in the Table 3. For sake of simplicity, the power devices and capacitors variations are assumed equal to the ones obtained for the full-bridge IGBTs and the dc-link capacitors, respectively. The inputs of the Monte-Carlo simulation are assumed to follow a normal distribution with a confidence interval of 99.7% (corresponding to 3σ).

Table 3: Maximum parameter variation used in the Monte Carlo simulation.

Maximum parameter variation	Power devices			Capacitors	
	A	ΔT_j	T_{jm}	L_0	T_h
(%)	20	10	5	15	10

Figure 5 (a) presents the component and system level unreliability curves for the 5-year mission profile. As observed, the full bridge IGBTs and the dc-link capacitors limit the inverter lifetime. Figure 5 (b) presents the component and system level unreliability curves for the TAY mission profile. As noted, the lifetime of the components is overestimated when the TAY mission profile is employed. When the averaging process is implemented, the mission profile extreme conditions are attenuated, i.e., the occurrences of high solar radiance and/or ambient temperature are diluted. Thus, maxima values are reduced and minima are increased, which also reduces the amplitudes of thermal cycles and helps to overestimate the lifetime of both capacitors and power devices. Moreover, the results for the power devices are more sensitive to the averaging process than the capacitors, since the damage in these devices is strongly dependent on the thermal cycle amplitudes.
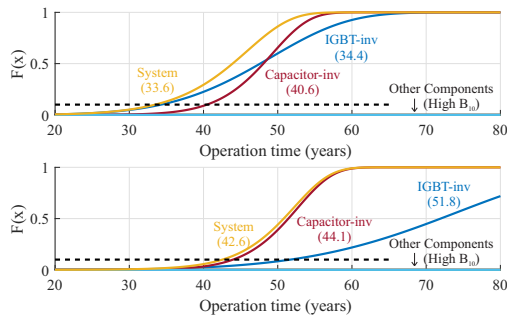
Figure 5: Component and system level unreliability function when the lifetime evaluation procedure employs: (a) 5-year mission profile; (b) TAY mission profile.

Figure 6 shows the effect of the mission profile length on the system level unreliability function. As previously discussed, the averaging process to compute the TAY mission profile always results in an overestimation of the converter lifetime. Moreover, the use of a reduced length mission profile also overestimates the PV inverter lifetime.

Finally, the B_{10} lifetime of the dc-link capacitors, inverter IGBTs and PV inverter are shown in Fig. 7. The TAY mission profile results in a system-level B_{10} lifetime estimation approximately 1.3 times higher than the continuously measured 5-year mission profile. Finally, the difference observed when different mission profile lengths are employed is lower than 7 %.
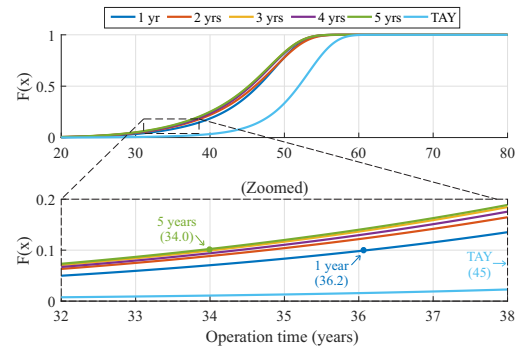
Figure 6: Effect of the mission profile length in the system level unreliability function.
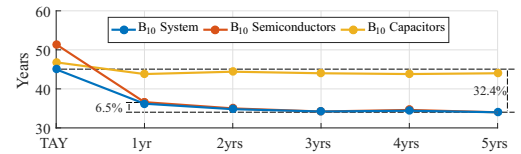
Figure 7: PV inverter B_{10} lifetime according to the mission profile length.

5. Conclusions

This paper analyzed the impact of the mission profile length on the lifetime evaluation of PV inverters. The performance of the measured data is compared with the typical average year approach. As observed, the averaging process attenuates the maximum and minimum weather conditions in the mission profile, reducing the thermal loading in the PV inverter components. This effect is even more relevant in the power modules, which are strongly dependent on the thermal cycling amplitudes.

The results show that when TAY is used in the reliability analysis, the lifetime prediction is increased

by 30% in comparison with the continuously measured 5-years mission profile. Therefore, the TAY is not recommended for this type of analysis.

On the other hand, the results indicate that the use of the 1-year mission profile results in a lifetime estimation lower than 7% when compared to a 5-years length mission profile. Despite the climatic randomness, the meteorological variation of the installation site did not result in a significant impact on the reliability analysis. Thus, it is preferred to use the mission profile data of one full year instead of the average multiple datasets. Notoriously, reduced mission profile lengths are preferred due to the computational effort needed to perform the lifetime evaluation.

6. Acknowledgement

References

[1] L.M.Moore, H. N. Post, Five years of operating experience at a large, utility-scale photovoltaic generating plant, Progress In Photovoltaics: Research And Applications 16 (3) (2008) 249–259.

[2] S. Yang, A. Bryant, P. Mawby, D. Xiang, L. Ran, P. Tavner, An industry-based survey of reliability in power electronic converters, IEEE Trans. Ind. Appl. 47 (3) (2011) 1441–1451.

[3] J. Falck, C. Felgemacher, A. Rojko, M. Liserre, P. Zacharias, Reliability of power electronic systems: An industry perspective, IEEE Ind. Electron. Mag. 12 (2) (2018) 24–35.

[4] A. Sangwongwanich, D. Zhou, E. Liivik, F. Blaabjerg, Mission profile resolution impacts on the thermal stress and reliability of power devices in pv inverters, Microelectronics Reliability 88-90 (2018) 1003 – 1007.

[5] H. Wang, M. Liserre, F. Blaabjerg, Toward reliable power electronics: Challenges, design tools, and opportunities, IEEE Ind. Electron. Mag. 7 (2) (2013) 17–26.

[6] U. Choi, K. Ma, F. Blaabjerg, Validation of lifetime prediction of igbt modules based on linear damage accumulation by means of superimposed power cycling tests, IEEE Trans. Ind. Electron. 65 (4) (2018) 3520–3529.

[7] P. D. Reigosa, H. Wang, Y. Yang, F. Blaabjerg, Prediction of bond wire fatigue of igbts in a pv inverter under a long-term operation, IEEE Trans. Power Electron. 31 (10) (2016) 7171–7182.

[8] A. Sangwongwanich, Y. Yang, D. Sera, F. Blaabjerg, Lifetime evaluation of grid-connected pv inverters considering panel degradation rates and installation sites, IEEE Trans. Power Electron. 33 (2) (2018) 1225–1236.

[9] A. Sangwongwanich, Y. Yang, D. Sera, F. Blaabjerg, D. Zhou, On the impacts of pv array sizing on the inverter reliability and lifetime, IEEE Trans. Ind. Appl 54 (4) (2018) 3656–3667.

[10] A. Sangwongwanich, E. Liivik, F. Blaabjerg, Photovoltaic module characteristic influence on reliability of micro-inverters, in: 2018 IEEE CPE-POWERENG, 2018, pp. 1–6.

[11] A. Sangwongwanich, Y. Yang, D. Sera, F. Blaabjerg, Mission profile-oriented control for reliability and lifetime of photovoltaic inverters, in: 2018 IPEC-ECCE, 2018, pp. 2512–2518.

[12] Y. Shen, A. Chub, H. Wang, D. Vinnikov, E. Liivik, F. Blaabjerg, Wear-out failure analysis of an impedance-source pv microinverter based on system-level electrothermal modeling, IEEE Trans. Ind. Electron. 66 (5) (2019) 3914–3927.

[13] J. M. Lenz, H. C. Sartori, J. R. Pinheiro, Mission profile characterization of pv systems for the specification of power converter design requirements, Solar Energy 157 (2017) 263 – 276.

[14] E. Brito, A. Cupertino, P. Reigosa, Y. Yang, V. Mendes, H. Pereira, Impact of meteorological variations on the lifetime of grid-connected pv inverters, Microelectronics Reliability 88-90 (2018) 1019 – 1024.

[15] Infineon Technologies AG, IKW20N60T Datasheet, rev. 2.8 (05 2015).

[16] K. Ma, F. Blaabjerg, Reliability-cost models for the power switching devices of wind power converters, in: 2012 PEDG, 2012, pp. 820–827.

[17] U. Scheuermann, R. Schmidt, P. Newman, Power cycling testing with different load pulse durations, in: 2014 PEMD, 2014, pp. 1–6.

[18] H. Wang, F. Blaabjerg, Reliability of capacitors for dc-link applications in power electronic converters—an overview, IEEE Trans. Ind. Appl. 50 (5) (2014) 3569–3578.

[19] Y. Yang, K. Ma, H. Wang, F. Blaabjerg, Instantaneous thermal modeling of the dc-link capacitor in photovoltaic systems, in: 2015 IEEE APEC, 2015, pp. 2733–2739.

[20] H. Niu, S. Wang, X. Ye, H. Wang, F. Blaabjerg, Lifetime prediction of aluminum electrolytic capacitors in led drivers considering parameter shifts, Microelectronics Reliability 88-90 (2018) 453 – 457.